PERIÓDICO TCHÊ QUÍMICA
ARTIGO ORIGINAL

ADSORÇÃO DE METAIS PESADOS A PARTIR DE UMA SOLUÇÃO MULTIMETAIS POR PELLETS DE ZEÓLITAS DE BENTONITA-CAOLIM: REGRESSÃO LINEAR E NÃO LINEAR E ANÁLISE DE ERROS

HEAVY METAL ADSORPTION FROM A MULTIMETAL SOLUTION BY BENTONITE-KAOLIN-ZEOLITE PELLETS: LINEAR AND NONLINEAR REGRESSION, AND ERROR ANALYSIS

ADSORCIÓN DE METALES PESADOS DE UNA SOLUCIÓN MULTIMETÁLICA USANDO PELLETS DE BENTONITA-CAOLÍN-ZEOLITA: REGRESIÓN LINEAL Y NO LINEAL, Y FUNCIONES DE ERROR

CARBONEL-RAMOS, Dalia Elisa[1*]; CHIRINOS, Hugo David[2]; AGARWAL, Madhu[3].

[1,2] National University of Engineering, Faculty of Environmental Engineering, Peru

[3] Department of Chemical Engineering, Malaviya National Institute of Technology Jaipur, India

** Correspondence author*
e-mail: dcarbonelr@uni.pe

Received 18 January 2020; received in revised form 05 February 2021; accepted 10 February 2021

RESUMO

Introdução: A poluição por metais pesados tem grandes impactos na saúde e nos ecossistemas; tecnologias de remediação podem reduzir custos para resolver esses problemas. Os metais pesados representam um sério problema no meio ambiente principalmente por sua tendência a persistir, bioacumular e biomagnificar na cadeia trófica. Remover esses compostos tóxicos das águas residuais ainda é uma tarefa desafiadora. **Objetivo:** A capacidade de remoção de metais pesados foi analisada usando pelotas adsorventes feitas com bentonita natural, caulim e zeólita. Este estudo descreve o equilíbrio de adsorção e cinética de remoção de metal usando análise de regressão linear e não linear. Os mecanismos de adsorção também foram analisados. **Métodos:** A qualidade do ajuste dos dados de equilíbrio de adsorção foi testada com as quatro formas linearizadas da equação de Langmuir, bem como os modelos de Freundlich, Temkin e Dubinin-Radushkevich. Para escolher o modelo de melhor ajuste com maior confiabilidade, cinco funções de erro foram utilizadas: R^2, X^2, SSE, ABS e ARE. Para a cinética de adsorção os modelos de Pseudo Primeira Ordem, Pseudo Segunda Ordem e Elovich foram estudados com análise de regressão linear e não linear. **Resultados e Discussão:** A linearização tipo I da isoterma de Langmuir deu o melhor ajuste para os três metais, com capacidades máximas de adsorção para chumbo, cobre e cádmio de 7,27, 1,45 e 0,28 mg/L respectivamente. Os resultados mostram que a Pseudo Segunda Ordem com regressão linear melhor ajustada para dados de chumbo e cobre e o modelo Pseudo Primeira Ordem com regressão linear para cádmio. **Conclusões:** A regressão não linear foi considerada melhor para se ajustar aos modelos de equilíbrio de adsorção e a regressão linear para se ajustar aos modelos cinéticos. Os principais mecanismos responsáveis pela adsorção no sistema são pensados para ser a troca iônica entre grupos funcionais e cátions, e atração de carga superficial relacionada às forças de Van der Waals.

Palavras-chave: Aluminossilicatos; peletização; tratamento de água poluída.

ABSTRACT

Background: Heavy metal pollution has significant impacts on health and ecosystems; remediation technologies can reduce the cost to solve these problems. Heavy metals present a severe problem in the environment, mainly for their tendency to persist, bioaccumulate and biomagnification in the trophic chain. Removing these toxic compounds from wastewater remains a challenging task. **Aim:** Heavy metal removal capacity was analyzed using adsorbent pellets made with natural bentonite, kaolin, and zeolite. This study describes the equilibrium adsorption and kinetics of metal removal by using linear and nonlinear regression analysis. Adsorption mechanisms were also analyzed. **Methods:** The goodness of fit of the adsorption equilibrium data was tested with the four linearized forms of the Langmuir equation, as well as the Freundlich, Temkin, and Dubinin-Radushkevich models. To choose the best-fit model with greater reliability, five error functions were used: R^2, X^2, SSE, ABS, and ARE. For adsorption kinetics the Pseudo First Order, Pseudo Second Order and Elovich models were studied with linear and nonlinear regression analysis. **Results and Discussion:** Type I linearization of the Langmuir isotherm

showed the best fit for the three metals, with maximum adsorption capacities for lead, copper, and cadmium of 7.27, 1.45 and 0.28 mg/L, respectively. The results show that Pseudo Second Order with linear regression best fitted for lead and copper data and Pseudo First Order model with linear regression for cadmium. **Conclusions:** Nonlinear regression was found better to fit adsorption equilibrium models and linear regression to fit kinetics models. The main mechanisms responsible for adsorption in the system are thought to be ion exchange between functional groups and cations and surface charge attraction related to Van der Waals forces.

Keywords: Alluminosilicates; pelletization; wastewater treatment.

RESUMEN

Antecedentes: La contaminación con metales pesados tiene graves impactos en la salud y los ecosistemas, las tecnologías de remediación pueden reducir los costos asociados a la resolución de estos problemas. Los metales pesados son un problema ambiental principalmente por su tendencia a ser persistentes, bioacumularse y biomagnificarse en la cadena trófica. Remover estos compuestos tóxicos de las aguas residuales continúa siendo un reto. **Objetivo:** La capacidad de remoción de metales pesados se analizó empleando adsorbentes hechos con bentonita, caolín y zeolita natural. Este estudio describe la cinética y parámetros de remoción de metales usando el análisis de regresión lineal y no lineal. **Métodos:** El ajuste de datos al equilibrio de adsorción se comparó con las cuatro formas linearizadas de la ecuación de Langmuir, así como con los modelos de Freundlich, Temkin y Dubinin-Radushkevich. Para escoger el modelo de mejor ajuste con mayor confiabilidad, se aplicaron cinco funciones de error: R^2, X^2, SSE, ABS y ARE. Para la cinética de adsorción se estudiaron los modelos de Pseudo Primer Orden, Pseudo Segundo Orden y Elovich con análisis de regresión lineal y no lineal. **Resultados y discusiones:** La linearización Tipo I de la isoterma de Langmuir fue la de mejor ajuste para los tres metales, con capacidades máximas de adsorción para plomo, cobre y cadmio de 7.27, 1.45 y 0.28 mg/L respectivamente. Los resultados muestran que el modelo de Pseudo Segundo Orden con regresión lineal fue el de mejor ajuste para plomo y cobre, y que el modelo de Pseudo Primer Orden con regresión lineal fue el de mejor ajuste para el cadmio. **Conclusiones:** La regresión no lineal se ajustó mejor a los modelos de equilibrio de adsorción y la regresión lineal a los modelos cinéticos. Se podría inferir que los principales mecanismos responsables de la adsorción del sistema son el intercambio iónico entre grupo funcionales y cationes, y la atracción por carga superficial relacionada con las fuerzas de Van der Waals.

Palabras clave: Aluminosilicatos; peletización; tratamiento de aguas residuales.

1. INTRODUCTION:

Heavy metal pollution has major impacts on health and ecosystems, and applying prevention technologies could reduce the costs associated with alleviating these problems. Heavy metals have toxic characteristics that aggravate the environmental pollution problem, i.e. persistence, bioaccumulation, and biomagnification (Kurniawan, Ismadji, Soetaredjo, and Ayucitra, 2014). Thus, how effectively and intensely remove undesired metals from wastewater is a serious and challenging task. Various technology proposed to remove heavy metals i.e., chemical precipitation, ion exchange, membrane filtration, electrochemical treatment. Chemical precipitation, used as a primary treatment, generates large amounts of hazardous waste. Membrane technologies (i.e., electrodialysis, reverse osmosis) gives excellent potential in the treatment process but high installation, maintenance, and energy costs (Renu, Agarwal, and Singh, 2017). Adsorption has many advantages compared to other treatments (Zhao, Xu, Zhang, Rong, and Zeng, 2016); it is a simple and economical treatment process that can remove heavy metals and a wide range of other contaminants (Worch, 2012).

Among the available adsorbents, clays, zeolites, and aluminosilicates are classified as the promising ones for heavy metals removal from aqueous systems. This is partly because of their great cation exchange capacity, low cost, high availability, high specific surface area, selectivity and regeneration capacity (Ismadji, Soetaredjo, and Ayucitra, 2015; Kurniawan *et al*., 2014; Novikova and Belchinskaya, 2016).

Evaluation of the goodness of fit to any model and determination of the parameters will enable the possible adsorption mechanisms to be understood. This is best done using regression analysis, either linear or nonlinear depending on their mathematical nature. In linear regression, the experimental data are adjusted to the to the linear expression of the model. In nonlinear regression, the parameters come from the nonlinear form of the model, and linearization, and linearization is not needed (Foo and Hameed, 2010).

Linear regression is one of the most

commonly used methods, despite the non-linearity of the kinetic and isothermal models and the linear analysis (Gusain, Srivastava, Sillanpää, and Sharma, 2016). On the other hand, nonlinear regression is a powerful tool for analyzing scientific data – the errors generated in linear adjustment are reduced (Ghaffari *et al*., 2017; Khalid, Kazmib, Habibc, Jabeena, and Shahzadd, 2015).

The objective of this study was to examine the adsorption of lead, copper and cadmium on bentonite, kaolin and zeolite pellets and describe the kinetic of metal removal and parameters by using linear and nonlinear regression analysis. Adsorption mechanisms were also defined in this work.

2. MATERIALS AND METHODS:

2.1. Clay characterization

The kaolin, bentonite and zeolite all came from natural deposits – the kaolin and bentonite from Cajamarca in northern Peru, and the zeolite from New Mexico (Hydro Source).

The aluminosilicates were characterized by spectrometry before pelletization and FTIR analysis was done on the pellets. Adsorbent pellets were ground in an agate mortar. Subsequently about 100 mg of adsorbent powder was analyzed at room temperature (20.3 ºC) and 66% of relative humidity. The analysis was made using a Perkin Elmer Frontier MIR spectrometer, with a $4cm^{-1}$ resolution and a KBr pressed disc technique.

2.2. Reagents

The metallic reagents – lead nitrate ($Pb(NO_3)_2$), copper sulfate pentahydrate ($CuSO_4.5H_2O$), and standard cadmium solution (1,000 mg/L) – were supplied by Merck Laboratories. Multimetallic solutions were prepared by diluting the reagents in distilled water, and the pH was adjusted with H_2S0_4 or KOH. Standard solutions for lead, copper, and cadmium were elaborated in four different concentrations, diluting standard stock solutions of 1000 mg/L concentration. This allowed obtaining the calibration curve. After adsorption and without further filtration, heavy metal concentrations were measured with an atomic absorption spectrometer (Model AA-700, Shimadzu), using an acetylene/air flame. The detection limit of the mentioned equipment for the three metals was between 0.001 mg/L and 0.009 mg/L. Wavelength measures for lead, copper and cadmium were 217 nm, 324.8 nm, and 228.8 nm, respectively. The slit width for all metals was 0.7 nm.

2.3. Pelletization

The dried clays and zeolites were screened to a particle size below 33 µm. Each pellet contained 67% zeolite, 29% bentonite, and 4% kaolin. The pellets were made using an adapted form of the method described in Miranda *et al.* (2015). The zeolite, bentonite, and kaolin powder mix were made into a paste with distilled water and then kneaded and passed through a manual extruder to form pellets 5 ± 0.1 mm long x 2 mm diameter. These were dried and calcined following Ciosek *et al.* (Ciosek, Luk, Warner, and Warner, 2016). The pellets were oven-dried at 105 °C for 18 hours and then calcined at 600 °C for 6 hours, increasing the temperature at 5 °C/min.

2.4. Adsorption tests

2.4.1 Adsorption column

Adsorption was evaluated in a column using a system similar to that described by Salem and Sene (Salem and Akbari Sene, 2012). A total of 300 mL aliquots of the solution were circulated at 20 mL/min using a peristaltic pump. Experiments were conducted at different parameters, i.e., circulation time, pH, and initial heavy metals concentration.

These were dried and calcined following recommendations by Ciosek *et al.* (2016). The pellets were oven-dried at 105 °C for 18 hours and then calcined at 600 °C for 6 hours, increasing the temperature at 5 °C/min.

2.4.2 Removal efficiency and adsorption capacity

Removal efficiency ($\%R_{em}$) was determined using Equation 1:

$$\%R_{em} = \frac{C_o - C_e}{C_o} \cdot 100 \qquad \text{(Eq. 1)}$$

where C_o (mg/L) and C_e (mg/L) represent the initial and final concentrations of the heavy metals.

The equilibrium adsorption capacity, Q_e, (mg/g) was found with Equation 2:

$$Q_e = \frac{Co - C_e}{m} \cdot V \qquad \text{(Eq. 2)}$$

where C_e (mg/L) is the equilibrium concentration, m the total mass of adsorbent (g) and V the

volume (L) of solution.

2.5. Equilibrium and kinetic studies

Adsorption equilibrium tests were performed with 300 mL of multimetallic solution, an adsorbent dose of 15 g/L and pH 4.5 ± 0.5, for 160 minutes. Initial lead and copper concentrations were between 1.5 and 30 mg/L, and cadmium between 0.5 and 15 mg/L. The data were fitted to the Langmuir, Freundlich, Temkin, and Dubinin-Radushkevich (D-R) models.

The Langmuir model (Equation 3) was the first equation proposed to describe adsorption:

$$Q_e = \frac{Q_{max} \cdot K_L \cdot C_e}{1 + K_L \cdot C_e} \qquad \text{(Eq. 3)}$$

where Q_e (mg/g) is the amount of solute adsorbed onto the adsorbent surface in equilibrium conditions, Q_{max} (mg/g) the maximum removal capacity of the adsorbent, and K_L (L/mg) and C_e (mg/L) the parameters of affinity and equilibrium concentration of the solute. The separation factor, R_L, is calculated using Equation 4:

$$R_L = \frac{1}{1 + b \cdot C_o} \qquad \text{(Eq. 4)}$$

where C_o (mg/L) is the initial concentration and b the intercept of the nonlinear equation.

The Freundlich isotherm (Equation 5) is also one of the very early empirical adsorption equations:

$$Q_e = K_F \cdot C_e^{1/n} \qquad \text{(Eq. 5)}$$

where K_F ((mg/g).(L/mg)^(1/n)) indicates the adsorption capacity of the adsorbent and n the system's heterogeneity.

The Temkin model is represented in Equation 6:

$$Q_e = B_T \cdot \ln(A_T \cdot C_e) \qquad \text{(Eq. 6)}$$

where A_T and B_T are equilibrium binding and parameter constants.

The D-R model is expressed in Equation 7:

$$Q_e = Q_{max} \cdot e^{-\beta\varepsilon^2} \qquad \text{(Eq. 7)}$$

β indicates the average sorption of free energy E (kJ/mol).

To analyze the adsorption kinetics, 500 mL portions of multimetallic solution were prepared, with initial Cu and Pb concentrations of 15 mg/L, and 5 mg-Cd/ L, an adsorbent dose of 10 g/L and pH 4 ± 0.5. Samples of the treated solution were taken between minutes 10 and 300. The pseudo first order (PFO), pseudo second order (PSO) and Elovich models were all analyzed. The PFO model (Equation 8) was proposed by Lagergren:

$$Q_t = Q_e(1 - \exp(k_1 \cdot T)) \qquad \text{(Eq. 8)}$$

where k_1 (1/min) and Q_e (mg/g) are parameter constants.

The PSO model, developed by Ho and McKay, is shown in Equation 9:

$$Q_t = \frac{Q_e^2 \cdot k_2 \cdot T}{1 + Q_e \cdot k_2 \cdot T} \qquad \text{(Eq. 9)}$$

where k_2 (g.mg^-1.min^-1) is the equation parameter.

Zeldowitsch developed the Elovich model (Equation 10):

$$Q_t = \frac{1}{Q_t} \ln((1 + Q_e \cdot k_e \cdot T) \qquad \text{(Eq. 10)}$$

where k_e (1/min) is the desorption constant.

2.6 Statistical analysis

For linear regression, the data were plotted according to the linearized form of each model (Table 1). It is noted that the Langmuir model can be linearized in four ways. The intercept and slope values on the graph were calculated, and the parameters for each equation were determined.

Table 1. *Linear expressions of Langmuir model*

Langmuir model	Linearization
Type I	$\frac{1}{Q_e} = \frac{1}{Q_{max} \cdot K_L} \cdot \frac{1}{C_e} + \frac{1}{Q_{max}}$
Type II	$\frac{C_e}{Q_e} = \frac{1}{Q_{max} \cdot K_L} + \frac{Ce}{Q_{max}}$
Type III	$Q_e = Q_{max} - \frac{1}{K_L} \cdot \frac{Q_e}{C_e}$

Type IV	$\frac{Q_e}{C_e} = KLQ_{max} - KLQ_e$

The nonlinear regression was optimized using the Excel Solver plug-in, with the GRG algorithm. Goodness of fit was measured on the basis of five different error functions (Table 2).

Table 2. *Error functions*

Function name	Error function
Sum of square errors- SSE	$SSE = \sum_{i=1}^{n} (y_{i,exp} - y_{i,mod})^2$
Coefficient of determination – R^2	$R^2 = 1 - \frac{\sum_{i=1}^{n}(y_{i,exp} - y_{i,mod})^2}{\sum_{i=1}^{n}(y_{i,exp} - \overline{y_{i,exp}})^2} = 1 - \frac{SSE}{SST}$
Sum of absolute errors - ABS	$ABS = \sum_{i=1}^{n} \lvert y_{i,exp} - y_{i,mod} \rvert$
Chi square – X^2	$x^2 = \sum_{i=1}^{n} \frac{(y_{i,exp} - y_{i,mod})^2}{y_{i,mod}}$
Average relative error - ARE	$ARE = \frac{100}{n} \sum_{i=1}^{n} \left\lvert \frac{y_{i,exp} - y_{i,mod}}{y_{i,mod}} \right\rvert$

3. RESULTS AND DISCUSSION:

3.1 Adsorbent characterization

Table 3 shows the chemical composition of the bentonite, kaolin and zeolite adsorbents. The three minerals consist mainly of silica and alumina, with lesser amounts of calcium, magnesium, sodium and potassium oxides. This confirms the potential of these materials for use as adsorbents (Uddin, 2017). The sodium and potassium oxides concentrations, and the magnesium and calcium oxides represent the feldspar content (Krupskaya *et al*., 2019). The ignition loss values indicate that these materials have low carbonaceous matter and high mineral content (Uddin, 2017).

Table 3. *Chemical composition of the clays and zeolite*

Element	Bentonite	Kaolin	Zeolite
SiO_2	62.63%	44.60%	65.91%
Al_2O_3	17.10%	36.09%	10.60%
Fe_2O_3	3.53%	3.43%	3.03%
CaO	2.61%	1.29%	2.52%
MgO	0.61%	0.35%	0.18%
Na_2O	0.99%	0.30%	3.77%
K_2O	0.07%	0.19%	0.14%
TiO_2	0.53%	1.42%	0.17%
P_2O_5	0.03%	0.03%	0.07%
Loss off ignition	11.80%	12.30%	13.60%

Figure 1 shows the FTIR analysis in the spectrum range between 400 and 4000 cm^{-1}. No peaks were observed in the first region of the spectrum, between the 3500 and 1600 cm^{-1} bands, attributed to surface and internal hydroxyl group vibrations. The curve is flat from 2842.60 to 1626 cm^{-1}, a region attributed to the adsorption of water in aluminosilicates (Hofmeister and Bowey, 2006). In the last region there is higher band intensity, this corresponds to the vibration of the oxygen bonds with aluminum or silicon. For the latter, the peaks are at 1023.04 cm^{-1} (from T-O junctions where T can be either aluminum or silicon) and six peaks in the range 874.79 and 447.00 cm^{-1} (corresponding to the T-O-T vibrations) (Madejová, Gates, and Petit, 2017).

3.2 Langmuir linearization

Langmuir model can be linearized in four different types of equations (Table 1), giving different results according to the formula used. Table 4 shows the equation parameters and error functions for each type of Langmuir linearization – the values vary independently, increasing or reducing the error. Langmuir equation types I and II are those most used because the results of the adjusted equations have less error (Armagan and Toprak, 2013). Table 4 shows that equations types I and IV were the ones with the least error.

The type I Langmuir equation obtained the highest R^2 and lowest ABS and ARE for the three metals studied. Type II Langmuir equation represents the smallest X^2 and lowest SSE for lead and copper. Type III equation shows the lowest SSE for cadmium, and type IV equation shows, the lowest ABS for copper and cadmium. From Table 4, it can be concluded that the type I Langmuir equation had the better fit to data.

These results show the complexity of estimating isothermal parameters using linearization techniques (Armagan and Toprak, 2013). For example, the R^2 linearization values for

each type (Table 4) and the other three models (Table 5) are all different. For lead and copper, the Langmuir equations types II, III, and IV R^2 values suggest that the Freundlich model gives the best fit. For cadmium, taking into account only Langmuir types II, III, and IV R^2 values, the Temkin isotherm would be the best fit.

3.3 Equilibrium isotherms

Table 5 compares the error functions of equilibrium models with linear and nonlinear regression, allowing the model to fit the data better. The X^2 value for 0.95 probability and 6 degrees of freedom is 1.64; all values are less than or equal to 1 (Table 5).

When changing from linear to nonlinear analysis, the values changed in all cases, except with R^2 of Temkin, and only for cadmium with X^2. The latter is to be expected given the low variation and concentrations of the data. Długosz and Banach (Długosz and Banach, 2018) obtained similar results in their study of copper adsorption on vermiculite; the Temkin model's R^2 was the same linear and nonlinear analyses.

The tendency is that nonlinear regression analysis reduces the error difference between experimental and expected data (Table 5). Comparing the error function values obtained with linear and nonlinear regression shows that four error functions (X^2, SSE, ABS, and ARE) indicate that the Temkin model had the worst fit to the experimental data. Regarding the error function variation from linear to nonlinear analysis, R^2 increased, and ABS and ARE decreased in all cases. This supports the findings of several authors who confirm that nonlinear regression analysis gives better results (Rostami, Pourzamani, Bina, and Karimi, 2019).

The differences between experimental data and the linear expressions of isotherms may be due to problems in the transformation from a nonlinear form, which is how adsorption models are expressed and formulated to a linear one. This changes the experimental error and the normality assumption in the least-squares. In linear regression the linearity of the points is assumed but not tested, and the slope and intercept of the best fit are predicted. The linear method assumes that the scattered points around this straight line have a Gaussian distribution and that the error distribution is the same for each value of "x". However, this rarely occurs in adsorption equilibrium models, where the distribution error is altered by transforming the data to linear form. In the linear method "y" is predicted for the corresponding "x" and only the error distribution along the "y" axis is considered, without taking into account its correspondence on the "x" axis (Armagan and Toprak, 2013). This yields different error values and parameters depending on how the data are linearized. For this reason, as well as on the evidence of the results from this study, nonlinear regression is considered the best method for determining equilibrium model adsorption parameters.

The linear regression error functions show that the Temkin model had the lowest R^2, and the highest SSE and ABS. For lead, the Langmuir model had the highest R^2, and the lowest SSE and ABS, while, for copper, the Freundlich model had the highest R^2 and lowest SSE (0.95 and 5.22), and the Langmuir model the highest R^2 and lowest ABS (0.98 and 0.48). Cadmium had higher and lowered R^2 and X^2 in the Temkin model with linear regression, but four error functions indicate that the Langmuir model best represents the data. For lead, R2, SSE, and ABS values confirm that the Langmuir isotherm is the best fit, while R^2 and ABS confirm the same for copper.

Error functions in the linear regression confirm that the Langmuir model best fits the lead, copper, and cadmium adsorption data, followed by the Freundlich model. Similar studies in which linear and nonlinear regression have been compared have had better results with linear analysis of the Langmuir model (Mallakpour and Rashidimoghadam, 2019), and sometimes with Freundlich, Temkin and D-R models (Batool, Akbar, Iqbal, Noreen, and Bukhari, 2018).

Figure 2 shows the Langmuir, Freundlich, Temkin, and D-R experimental data and nonlinear regression curves models. It is notorious the better fit of data to Langmuir and Freundlich models for the three metals.

Table 6 shows the parameters and R^2 values for each model for linear and nonlinear analyses, and the great variation between the Langmuir linear and nonlinear parameters model for lead, copper and cadmium is evident.

3.3.1 Langmuir

The error function analysis for lead, copper and cadmium in the nonlinear regression indicates that the Langmuir model best describes the experimental data. Other authors have obtained similar results with heavy metal adsorption onto clays (K. Abu-Hawwas, M. Ibrahim, and M. Musleh, 2018; Mu'azu, Bukhari, and Munef, 2020). The maximum adsorption capacities predicted by the Langmuir model for lead, copper, and

cadmium are 7.27, 1.45, and 0.68 mg/g, respectively. The best fit by the Langmuir model means that the process occurs in a monolayer and that each active site houses an adsorbate molecule, characteristics typical of physisorption (Ismadji *et al*., 2015).

The parameter K_L measures the adsorption intensity between the adsorbate and adsorbent (Ismadji *et al*., 2015). In this study its value was highest for cadmium and lowest for lead, implying that cadmium molecule adhesion at the interface is stronger than that of copper and lead. The separation factor, R_L, indicates the viability of adsorption (Ismadji *et al*., 2015). Table 6 observed that this factor was reduced from a linear to a nonlinear regression; however, for the three metals, the ranges remained lower than 1, indicating that the adsorption is viable.

3.3.2 Freundlich

In the Freundlich model, the parameter K_F is related to multilayer adsorption capacity, and n indicates adsorption intensity, which varies with interface heterogeneity (Ismadji *et al*., 2015). The value of n enables understanding of the process and the system's complexity; magnitudes between 1 and 10 are considered favorable, but values exceeding 10 indicate irreversible conditions. Nonlinear regression for lead, copper, and cadmium yielded values of 1.09, 3.30, and 6.09, respectively, showing that the process is viable, with adsorption tending to be most substantial for cadmium, then copper, and finally lead. K_F also indicates the sorption capacity of the adsorbent (Ismadji *et al*., 2015). It was highest for copper, followed by lead and cadmium. These results agree with Bahabadi *et al.* (Bahabadi, Farpoor, and Mehrizi, 2017). They studied adsorption on clays and zeolites and concluded that natural adsorbents had a greater affinity for copper than zinc and cadmium.

The nonlinear analysis of R^2 showed that the Freundlich model is second in order adjustment for lead and cadmium, and third for copper. Similar results were reported by Soleimani and Siahpoosh (Soleimani and Siahpoosh, 2015) in relation to copper adsorption with nanoclays. While the Freundlich model is not the best to describe the data, the values of R^2, between 0.968 and 0.986, indicate that the equation may be applicable. This can be attributed to the fact that active sites can be characterized as monolayer or multilayer, and the interface as heterogeneous (Padmavathy and Murali, 2017).

3.3.3 Temkin

Low Q_t values for the three metals studied indicate that adsorption is physical. The A_T value decreased in the order Cd>Cu>Pb, indicating that cadmium has the highest binding energy of the three to the adsorbent. This corroborates the results from the Freundlich and Langmuir models.

According to the nonlinear R^2, the Temkin model had the lowest fit for lead, copper, and cadmium. This behavior is common in adsorption studies (Salmani *et al*., 2019). The results agree with the data fit to the Langmuir model, indicating the predominance of physisorption. The Temkin isotherm is more appropriate for describing chemisorption (Ahmedzeki, Rashid, Alnaama, Alhasani, and Abdulhussain, 2013; Gao *et al*., 2013).

3.3.4 D-R

The D-R model helps to distinguish between physical and chemical adsorption using the value of E. When this is below 8 kJ/mol, adsorption is physical; between 8 and 16 kJ/mol ion exchange and chemical mechanisms predominate; and above 16 kJ/mol, particle diffusion governs the reaction (Sadeghalvad, Khosravi, and Azadmehr, 2016). Table 6 shows that E is reduced when transferring from linear to nonlinear analysis, except below 8 kJ/mol, where values were maintained, indicating physical adsorption. This corroborates the findings from the three other models.

For lead and cadmium, the nonlinear R^2 places this model third in order of adjustment, consistent with several studies showing lower R^2 values with this equation (Mosai and Tutu, 2019; Nikolic, Jeffry Robert, and Girish, 2019).

3.4 Kinetics

Experimental data were compared with three equations that consider surface reaction kinetics as a critical step: the PFO, PSO, and Elovich models. The linear regressions for the three, and their respective equations, are shown in Figure 3.

When changing from linear to nonlinear regression (Table 7) the error functions all vary except X^2 in the PFO model and X^2 and R^2 in the PSO model for lead. Variations are expected when moving between linear and nonlinear models – e.g., López-Luna *et al.* (López-Luna *et al*., 2019) had similar outcomes in a study of arsenic and manganese adsorption.

Having five error functions to select the best fit increases the reliability of the results. For 9 degrees of freedom and p 0.95, X^2 is 3.33. Table 7 shows no data exceeded this limit, even for p 0.99 (X^2 is 2.09). A comparison shows that SSE, ABS, and ARE for lead, copper, and cadmium are higher in the Elovich equation.

When changing from linear to nonlinear regression concerning error function, R^2 increased in all cases, except for the PSO model for lead. X^2 decreased for copper and cadmium in all three models, but for lead, it remained the same in the PFO and PFO models and increased in the Elovich model. SSE decreased in all cases, and ARE was reduced in the PFO model for lead, and in the Elovich model for both lead and copper.

The error function analysis seems to indicate error reduction with nonlinear regression. However, the optimal parameter values for cadmium could not be found for the PFO model when performing nonlinear regression and some parameter values suggested during optimization were very low (Table 8). The Elovich nonlinear parameters, Q_e, are much lower than both the linear and experimental parameters, which means that nonlinear regression cannot be applied successfully to the Elovich model. Moreover, the lead and copper error functions and parameters are similar in the linear and nonlinear regressions. The Elovich model's inapplicability and the small difference between linear and nonlinear regression for lead and copper meant that kinetic analysis was preferred using linear regression. Other authors have reported similar results (Açikyildiz, Gürses, Güneş, and Yalvaç, 2015). Nonlinear regression for kinetic models demands specific and previous expertise and takes longer (Açıkyıldız *et al.*, 2015).

The best fit for cadmium was the PFO model in linear and nonlinear regression (Table 7). Lead and copper showed best fits with the PSO model with linear regression, and this was maintained in nonlinear regression for lead. Other authors have also reported good correlations with these models (Milenković *et al*., 2013) and a poorer fit with the Elovich equation (Yousefi *et al*., 2018).

Figure 4 shows linear regression curves of the PFO, PSO, and Elovich models.

3.4.1 PFO

The PFO model is widely used to describe the heavy metal adsorption but the adsorption capacity predicted is usually below the experimental one (Dotto, Salau, Piccin, Cadaval, and de Pinto, 2017). The Q_e values for lead, copper, and cadmium are 0.95, 0.94, and 0.85 mg/g, respectively. Those for lead and copper are lower than the experimental maxima for both linear and nonlinear regressions.

In the case of cadmium, in both linear and nonlinear regressions, the error functions indicate that the PFO model is the best fit. In this model, it is assumed that the adsorption rate is directly proportional to the adsorbate concentration and that the limiting step is diffusion at the adsorption surface (Ho and McKay, 1999). Although it is most common that the PSO model gives the best fit to the data in heavy metal adsorption, other researchers have reported similar results (Mejia Miranda, Laverde, Avella, and Peña Ballesteros, 2015).

3.4.2 PSO

Ho and McKay (1999) suggested that, if metal ion adsorption fits the PSO model, the process limiting step could be chemisorption. This would involve adsorbate-adsorbent electron exchange, although physical interactions could also be the cause.

In both linear and nonlinear regression analysis, lead fits the PSO model best, and the same is true for copper in linear regression. Several heavy metal adsorption studies with bentonite and zeolite, have shown a better fit to the PSO model (Melichová and Ľuptáková, 2016; Mu'azu *et al*., 2020). The results seem to indicate that chemisorption could control lead and copper adsorption.

3.4.3 Elovich

The calculated adsorption capacity of metals was lower than the experimental one due to this the Elovich equation for linear and non linear regression was not suitable to describe adsorption capacity of three metals.

Although the model has been reported to adjust better at very low concentrations (López-Luna *et al*., 2019), it is usual for this equation to have a lower adjustment of data than the PFO PSO models (Schwantes *et al*., 2016).

3.5 Adsorption mechanisms

After selecting the appropriate adsorbent in terms of cost, efficiency, selectivity and kinetics, the second most important step for effective adsorption is to identify the predominant

mechanisms and elucidate the interactions occurring at the interface.

Adsorption mechanisms can be classified into physisorption, ion exchange, chemisorption, and precipitation. Physisorption includes processes like surface adsorption, Van der Waals interactions and hydrogen bonding (Crini, Lichtfouse, Wilson, and Morin-Crini, 2018). Ion exchange involves replacing interchangeable cations (i.e. Na+, K+, Ca^2+ and Mg^2+) at the interface, and is usually fast and reversible (Shaban and Abukhadra, 2017), but also between the aluminosilicate Al(OH) and Si(OH) groups and the metal ions (Burakov *et al*., 2018). Chemisorption usually involves electrostatic interactions, covalent bonds, and complex formation, while precipitation can be micro- or surface-, or via proton displacement (Crini *et al.*, 2018). Several authors agree that the above are all likely mechanisms in natural adsorbents (Al-Jlil and Latif, 2013; Alexander, Ahmad Zaini, Surajudeen, Aliyu, and Omeiza, 2018).

The analysis carried out in the investigation did not cover complex formation or surface precipitation in the adsorbent; for this reason, it is unknown if these mechanisms also play an important role in adsorption.

Adsorption equilibrium and kinetics analysis indicate the predominance of physisorption in the system. Therefore, it can be deduced that the main mechanisms responsible for adsorption are: ion exchange between functional groups and cations and surface charge attraction related to Van der Waals forces.

4. CONCLUSIONS:

Nonlinear regression was found better to fit adsorption equilibrium models and linear regression to fit kinetics models. The Langmuir isotherm gave the best fit to the experimental data with maximum adsorption capacities for lead, copper, and cadmium of 7.27, 1.45, and 0.28 mg/L, respectively. The Freundlich isotherm also had high correlation values (R^2 between 0.968 and 0.986), indicating that active sites can be characterized as mono or multilayer, and the adsorption surface as heterogeneous. The lead and copper data were better adjusted to the PSO model, and the cadmium data to the PFO model.

5. ACKNOWLEDGMENTS:

This research was made with funding from the Faculty of Environmental Engineering of the National University of Engineering in Peru (Grant Number RD 038-2018).

6. REFERENCES:

1. Açikyildiz, M., Gürses, A., Güneş, K., and Yalvaç, D. (2015). A comparative examination of the adsorption mechanism of an anionic textile dye (RBY 3GL) onto the powdered activated carbon (PAC) using various the isotherm models and kinetics equations with linear and nonlinear methods. *Applied Surface Science*. https://doi.org/10.1016/j.apsusc.2015.07.021
2. Ahmedzeki, N. S., Rashid, H. A., Alnaama, A. A., Alhasani, M. H., and Abdulhussain, Z. (2013). Removal of 4-nitro-phenol from wastewater using synthetic zeolite and kaolin clay. *Korean Journal of Chemical Engineering*, *30*(12), 2213–2218. https://doi.org/10.1007/s11814-013-0165-x
3. Al-Jlil, S. A., and Latif, M. S. (2013). Evaluation of equilibrium isotherm models for the adsorption of Cu and Ni from wastewater on bentonite clay. *Materiali in Tehnologije*.
4. Alexander, J. A., Ahmad Zaini, M. A., Surajudeen, A., Aliyu, E. N. U., and Omeiza, A. U. (2018). Insight into kinetics and thermodynamics properties of multicomponent lead(II), cadmium(II) and manganese(II) adsorption onto Dijah-Monkin bentonite clay. *Particulate Science and Technology*. https://doi.org/10.1080/02726351.2016.1276499
5. Armagan, B., and Toprak, F. (2013). Optimum isotherm parameters for reactive azo dye onto pistachio nut shells: Comparison of linear and nonlinear methods. *Polish Journal of Environmental Studies*.
6. Bahabadi, F. N., Farpoor, M. H., and Mehrizi, M. H. (2017). Removal of Cd, Cu and Zn ions from aqueous solutions using natural and Fe modified sepiolite, zeolite and palygorskite clay minerals. *Water Science and Technology*. https://doi.org/10.2166/wst.2016.522
7. Batool, F., Akbar, J., Iqbal, S., Noreen, S., and Bukhari, S. N. A. (2018). Study of

Isothermal, Kinetic, and Thermodynamic Parameters for Adsorption of Cadmium: An Overview of Linear and Nonlinear Approach and Error Analysis. *Bioinorganic Chemistry and Applications*. https://doi.org/10.1155/2018/3463724

8. Burakov, A. E., Galunin, E. V., Burakova, I. V., Kucherova, A. E., Agarwal, S., Tkachev, A. G., and Gupta, V. K. (2018). Adsorption of heavy metals on conventional and nanostructured materials for wastewater treatment purposes: A review. *Ecotoxicology and Environmental Safety*, *148*, 702–712. https://doi.org/10.1016/j.ecoenv.2017.11.034
9. Ciosek, A. L., Luk, G. K., Warner, M., and Warner, R. A. (2016). An Innovative Design of a Clay-Zeolite Medium for the Adsorption of Total Phosphorus from Wastewater. *Water Environment Research*, *88*(2), 131–142. https://doi.org/10.2175/106143015X14338845155787
10. Crini, G., Lichtfouse, E., Wilson, L. D., and Morin-Crini, N. (2018). *Adsorption-Oriented Processes Using Conventional and Non-conventional Adsorbents for Wastewater Treatment*. https://doi.org/10.1007/978-3-319-92111-2_2
11. Długosz, O., and Banach, M. (2018). Kinetic, isotherm and thermodynamic investigations of the adsorption of Ag+ and Cu2+ on vermiculite. *Journal of Molecular Liquids*, *258*, 295–309. https://doi.org/10.1016/j.molliq.2018.03.041
12. Dotto, G. L., Salau, N. P. G., Piccin, J. S., Cadaval, T. R. S., and de Pinto, L. A. A. (2017). Adsorption Kinetics in Liquid Phase: Modeling for Discontinuous and Continuous Systems. In *Adsorption Processes for Water Treatment and Purification* (pp. 53–76). https://doi.org/10.1007/978-3-319-58136-1_3
13. Foo, K. Y., and Hameed, B. H. (2010). Insights into the modeling of adsorption isotherm systems. *Chemical Engineering Journal*, *156*(1), 2–10. https://doi.org/10.1016/j.cej.2009.09.013
14. Gao, Y., Chen, N., Hu, W., Feng, C., Zhang, B., Ning, Q., and Xu, B. (2013). Phosphate Removal from Aqueous Solution by an Effective Clay Composite Material. *Journal of Solution Chemistry*, *42*(4), 691–704. https://doi.org/10.1007/s10953-013-9985-x
15. Ghaffari, H. R., Pasalari, H., Tajvar, A., Dindarloo, K., Goudarzi, B., Alipour, V., and Ghanbarneajd, A. (2017). Linear and nonlinear two-parameter adsorption isotherm modeling: a case-study. *Int. J. Eng. Sci.*, *6*(9), 01–11.
16. Gusain, D., Srivastava, V., Sillanpää, M., and Sharma, Y. C. (2016). Kinetics and isotherm study on adsorption of chromium on nano crystalline iron oxide/hydroxide: linear and nonlinear analysis of isotherm and kinetic parameters. *Research on Chemical Intermediates*, *42*(9), 7133–7151. https://doi.org/10.1007/s11164-016-2523-x
17. Ho, Y. ., and McKay, G. (1999). Pseudo-second order model for sorption processes. *Process Biochemistry*, *34*(5), 451–465. https://doi.org/10.1016/S0032-9592(98)00112-5
18. Hofmeister, A. M., and Bowey, J. E. (2006). Quantitative Infrared Spectra of Hydrosilicates and Related Minerals. *Monthly Notices of the Royal Astronomical Society*, *367*(2), 577–591. https://doi.org/10.1111/j.1365-2966.2006.09894.x
19. Ismadji, S., Soetaredjo, F. E., and Ayucitra, A. (2015). *Clay Materials for Environmental Remediation*. https://doi.org/10.1007/978-3-319-16712-1
20. K. Abu-Hawwas, J., M. Ibrahim, K., and M. Musleh, S. (2018). Characterization of Jordanian Porcelanite Rock with Reference to the Adsorption Behavior of Lead Ions from Aqueous Solution. *Oriental Journal of Chemistry*, *34*(2), 663–674. https://doi.org/10.13005/ojc/340208
21. Khalid, A., Kazmib, M. ., Habibc, M., Jabeena, S., and Shahzadd, K. (2015). Kinetic and equilibrium modelling of copper biosorption. *Journal of Faculty of Engineering and Technology*, *22*(1), 131–145.
22. Krupskaya, V., Novikova, L., Tyupina, E., Belousov, P., Dorzhieva, O., Zakusin, S., … Belchinskaya, L. (2019). The influence

of acid modification on the structure of montmorillonites and surface properties of bentonites. *Applied Clay Science*, *172*, 1–10. https://doi.org/10.1016/j.clay.2019.02.001

23. Kurniawan, A., Ismadji, S., Soetaredjo, F. ., and Ayucitra, A. (2014). Natural clays/clay minerals and modified forms for heavy metals removal. In R. S. of Chemistry (Ed.), *Heavy Metals in Water: Presence, Removal and Safety* (First Edit, p. 380). Cambridge, United Kingdom.

24. López-Luna, J., Ramírez-Montes, L. E., Martinez-Vargas, S., Martínez, A. I., Mijangos-Ricardez, O. F., González-Chávez, M. del C. A., … Vázquez-Hipólito, V. (2019). Linear and nonlinear kinetic and isotherm adsorption models for arsenic removal by manganese ferrite nanoparticles. *SN Applied Sciences*, *1*(8), 950. https://doi.org/10.1007/s42452-019-0977-3

25. Madejová, J., Gates, W. P., and Petit, S. (2017). *IR Spectra of Clay Minerals*. https://doi.org/10.1016/B978-0-08-100355-8.00005-9

26. Mallakpour, S., and Rashidimoghadam, S. (2019). Poly(vinyl alcohol)/Vitamin C-multi walled carbon nanotubes composites and their applications for removal of methylene blue: Advanced comparison between linear and nonlinear forms of adsorption isotherms and kinetics models. *Polymer*, *160*, 115–125. https://doi.org/10.1016/j.polymer.2018.11.035

27. Mejia Miranda, C., Laverde, D., Avella, V., and Peña Ballesteros, D. Y. (2015). Adsorción de iones Ni(II) sobre una arcilla bentonítica peletizada. *Revista ION*, *28*(2), 61–68. https://doi.org/10.18273/revion.v28n2-2015005

28. Melichová, Z., and Ľuptáková, A. (2016). Removing lead from aqueous solutions using different low-cost abundant adsorbents. *Desalination and Water Treatment*, *57*(11), 5025–5034. https://doi.org/10.1080/19443994.2014.999713

29. Milenković, D., Milosavljević, M., Marinković, A., Đokić, V., Mitrović, J., and Bojić, A. L. (2013). Removal of copper(II) ion from aqueous solution by high-porosity activated carbon. *Water SA*, *39*(4). https://doi.org/10.4314/wsa.v39i4.10

30. Mosai, A. K., and Tutu, H. (2019). The effect of crop exudates and EDTA on cadmium adsorption by agricultural podsolic soil: implications on groundwater. *International Journal of Environmental Science and Technology*, *16*(7), 3071–3080. https://doi.org/10.1007/s13762-018-1927-0

31. Mu'azu, N. D., Bukhari, A., and Munef, K. (2020). Effect of montmorillonite content in natural Saudi Arabian clay on its adsorptive performance for single aqueous uptake of Cu(II) and Ni(II). *Journal of King Saud University - Science*, *32*(1), 412–422. https://doi.org/10.1016/j.jksus.2018.06.003

32. Nikolic, M., Jeffry Robert, R., and Girish, C. R. (2019). The Adsorption of Cadmium, Nickel, Zinc, Copper and Lead from Wastewater using Tea Fiber Waste. *Journal of Engineering and Applied Sciences*, *14*(20), 7743–7755. https://doi.org/10.36478/jeasci.2019.7743.7755

33. Novikova, L., and Belchinskaya, L. (2016). Adsorption of Industrial Pollutants by Natural and Modified Aluminosilicates. In *Clays, Clay Minerals and Ceramic Materials Based on Clay Minerals*. https://doi.org/10.5772/61678

34. Padmavathy, K., and Murali, A. (2017). Adsorption of hexavalent chromium (Cr (VI)) from wastewater using novel chitosan/halloysite clay nanocomposite films. *Indian Journal of Chemical Technology*, *24*(6), 593–600.

35. Renu, Agarwal, M., and Singh, K. (2017). Heavy metal removal from wastewater using various adsorbents: a review. *Journal of Water Reuse and Desalination*, *7*(4), 387–419. https://doi.org/10.2166/wrd.2016.104

36. Rostami, M., Pourzamani, H., Bina, B., and Karimi, H. (2019). Linear and nonlinear isotherm modeling of nitrate removal from aqueous solution by alternating current electrocoagulation. *International Journal of Environmental Health Engineering*, *8*(1), 2. https://doi.org/10.4103/ijehe.ijehe_9_17

37. Sadeghalvad, B., Khosravi, S., and Azadmehr, A. R. (2016). Nonlinear isotherm and kinetics of adsorption of

copper from aqueous solutions on bentonite. *Russian Journal of Physical Chemistry A*, *90*(11), 2285–2291. https://doi.org/10.1134/S00360244161100 30

38. Salem, A., and Akbari Sene, R. (2012). Optimization of zeolite-based adsorbent composition for fabricating reliable Raschig ring shaped by extrusion using Weibull statistical theory. *Microporous and Mesoporous Materials*, *163*, 65–75. https://doi.org/10.1016/j.micromeso.2012. 06.026
39. Salmani, M. H., Sahlabadi, F., Eslami, H., Ghaneian, M. T., Balaneji, I. R., and Zad, T. J. (2019). Removal of Cr(VI) oxoanion from contaminated water using granular jujube stems as a porous adsorbent. *Groundwater for Sustainable Development*, *8*, 319–323. https://doi.org/10.1016/j.gsd.2018.12.001
40. Schwantes, D., Gonçalves, A. C., Coelho, G. F., Campagnolo, M. A., Dragunski, D. C., Tarley, C. R. T., … Leismann, E. A. V. (2016). Chemical Modifications of Cassava Peel as Adsorbent Material for Metals Ions from Wastewater. *Journal of Chemistry*, *2016*, 1–15. https://doi.org/10.1155/2016/3694174
41. Shaban, M., and Abukhadra, M. R. (2017). Geochemical evaluation and environmental application of Yemeni natural zeolite as sorbent for Cd2+ from solution: kinetic modeling, equilibrium studies, and statistical optimization. *Environmental Earth Sciences*, *76*(8), 310. https://doi.org/10.1007/s12665-017-6636-3
42. Soleimani, M., and Siahpoosh, Z. H. (2015). Ghezeljeh nanoclay as a new natural adsorbent for the removal of copper and mercury ions: Equilibrium, kinetics and thermodynamics studies. *Chinese Journal of Chemical Engineering*, *23*(11), 1819–1833. https://doi.org/10.1016/j.cjche.2015.08.02 4
43. Uddin, M. K. (2017). A review on the adsorption of heavy metals by clay minerals, with special focus on the past decade. *Chemical Engineering Journal*, *308*, 438–462. https://doi.org/10.1016/j.cej.2016.09.029
44. Worch, E. (2012). *Adsorption technology in water treatment* (W. de Gruyter, ed.). Beriln.
45. Yousefi, T., Abas Mohsen, M., Mahmudian, H. R., Torab-Mostaeidi, M., Moosavian, M. A., and Aghayan, H. (2018). Removal of Pb(II) by Modified Natural Adsorbent; Thermodynamics and Kinetics Studies. *J. Water Environ. Nanotechnol*, *3*(3), 265–272. https://doi.org/10.22090/jwent.2018.03.00 7
46. Zhao, M., Xu, Y., Zhang, C., Rong, H., and Zeng, G. (2016). New trends in removing heavy metals from wastewater. *Applied Microbiology and Biotechnology*, *100*(15), 6509–6518. https://doi.org/10.1007/s00253-016-7646-x

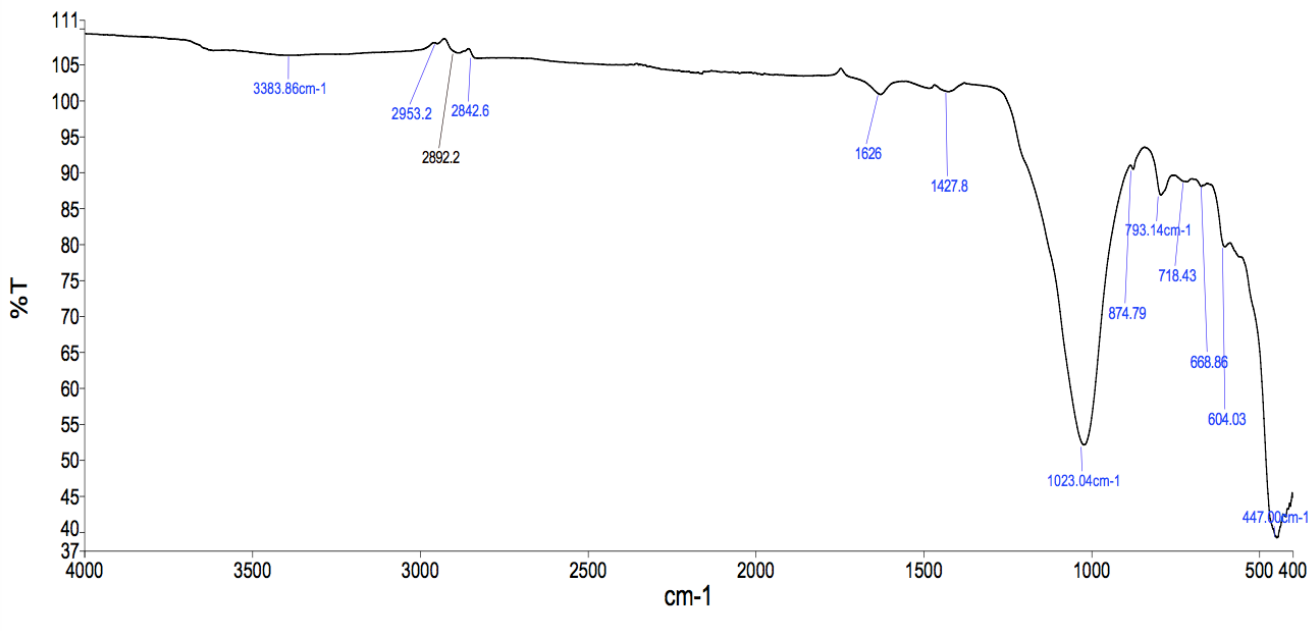

Figure 1. *FTIR spectra of adsorbent pellets*

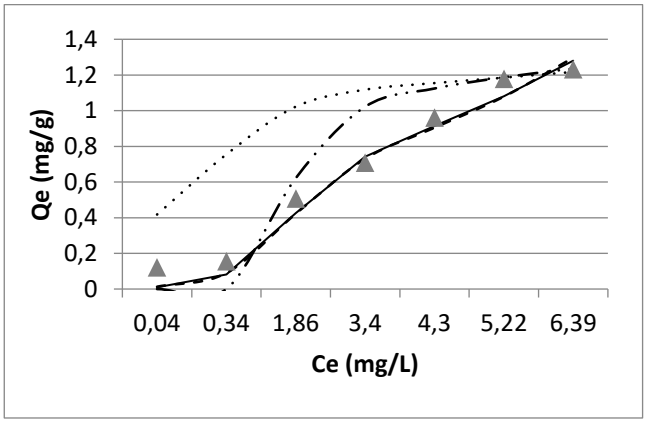

(a)

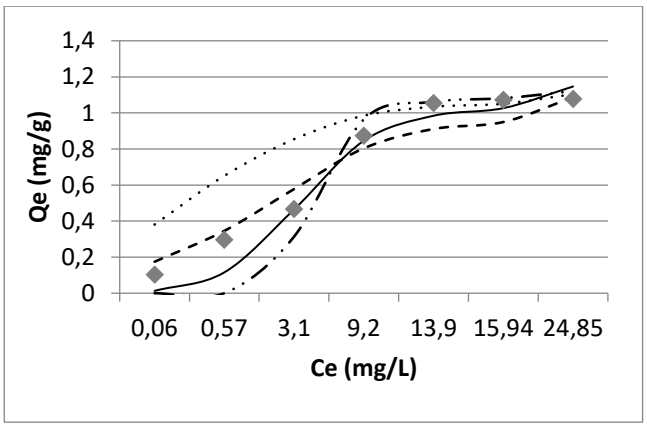

(b)

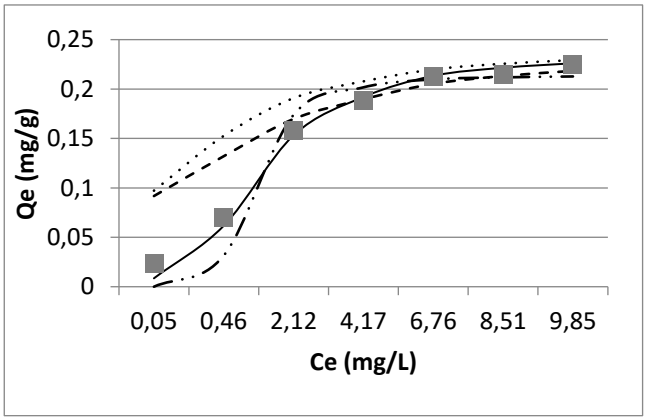

(c)

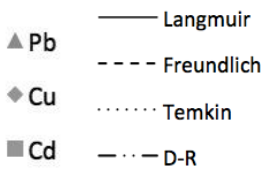

Figure 2. *Adsorption equilibrium curves with nonlinear regression for lead (a), copper (b), and cadmium (c)*

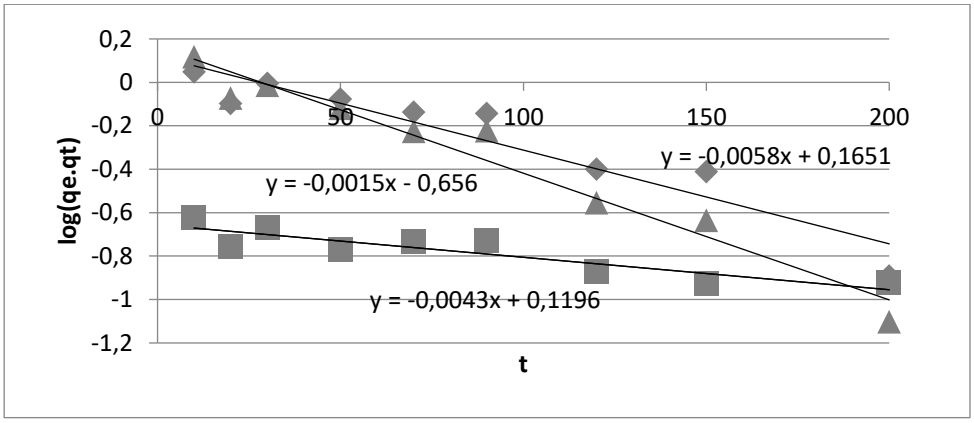

(a)

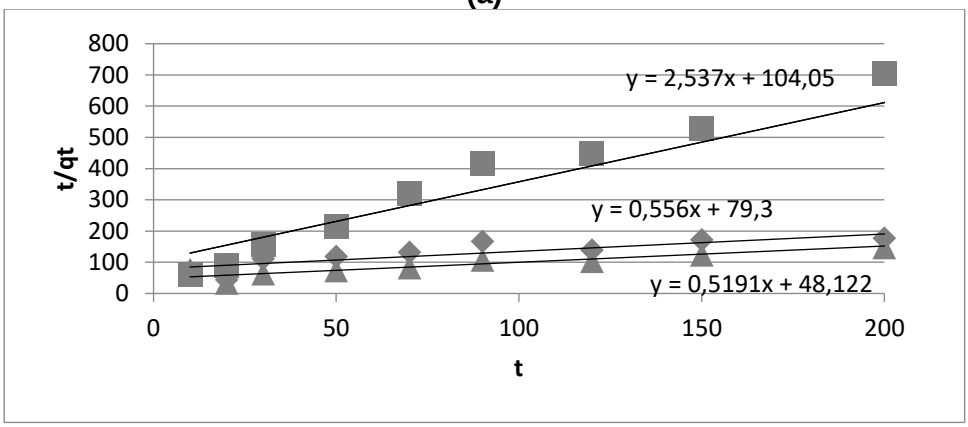

(b)

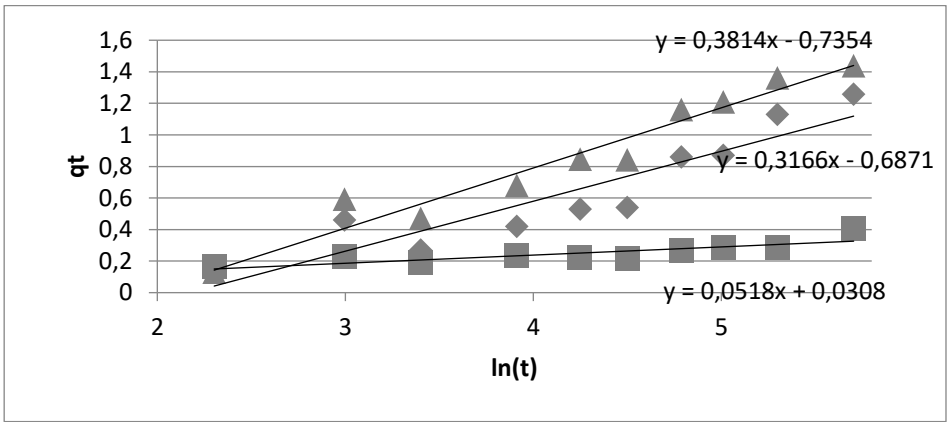

(c)

▲ Pb

◆ Cu

■ Cd

Figure 3. *Linear regression of PFO (a), PSO (b), and Elovich (c) models*

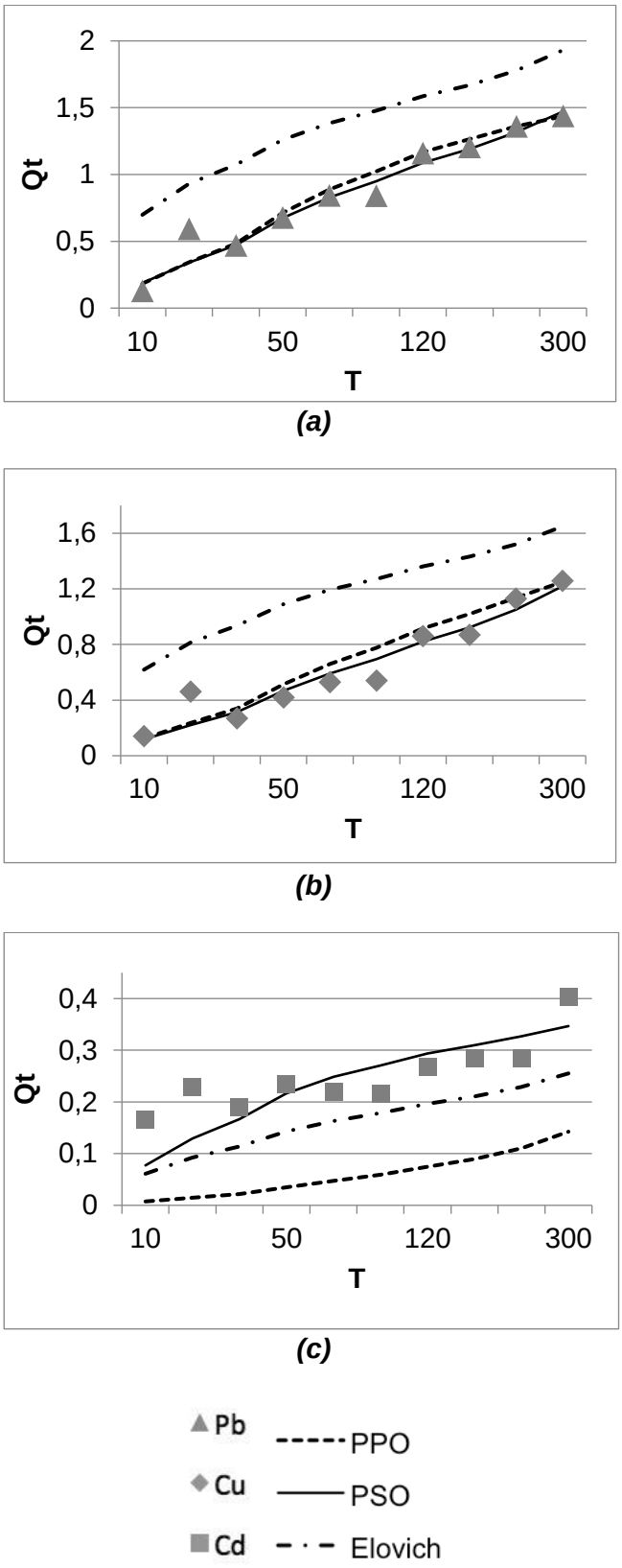

Figure 4. *Linear regression curves of kinetic models for lead (a), copper (b), and cadmium (c)*

Table 4. *Adsorption parameters and error functions for Langmuir equations type I, II, III and IV*

Model	Parameters	Pb	Cu	Cd
Langmuir Type I	Q_{max} (mg/g)	1.59	1.18	0.24
	K_L (L/mg)	0.38	0.43	1.07
	R^2	0.924	0.943	0.991
	X^2	1.000	1.000	1.000
	SSE	15.420	14.847	0.641
	ABS	0.720	0.499	0.046
	ARE	25.179	21.776	10.743
Langmuir Type II	Q_{max} (mg/g)	0.55	0.74	0.18
	K_L (L/mg)	6.68	2.64	2.92
	R^2	0.585	0.754	0.915
	X^2	0.971	0.754	0.915
	SSE	8.937	0.998	1.000
	ABS	2.180	10.802	0.539
	ARE	47.347	1.543	0.187
Langmuir Type III	Q_{max} (mg/g)	0.87	0.92	0.21
	K_L (L/mg)	3.79	1.85	2.26
	R^2	0.663	0.800	0.941
	X^2	0.981	0.999	1.000
	SSE	12.921	13.107	0.603
	ABS	1.582	1.057	0.114
	ARE	51.532	26.926	13.996
Langmuir Type IV	Q_{max} (mg/g)	1.16	1.03	0.22
	K_L (L/mg)	1.42	1.18	1.83
	R^2	0.793	0.853	0.960
	X^2	0.994	0.999	1.000
	SSE	15.597	14.423	0.625
	ABS	1.249	0.824	0.092
	ARE	46.458	25.498	13.377

Table 5. *Equilibrium models error functions of with linear and nonlinear regression*

Model		Lead		Copper		Cadmium	
		Linear	**Nonlinear**	**Linear**	**Nonlinear**	**Linear**	**Nonlinear**
Langmuir	R^2	0.585	0.987	0.754	0.981	0.915	0.999
	X^2	0.971	1	0.998	1	1	1
	SSE	8.937	15.168	10.802	14.275	0.539	0.638
	ABS	2.18	0.494	1.543	0.482	0.187	0.04
	ARE	47.347	25.354	29.728	24.127	17.385	12.043
Freundlich	R^2	0.953	0.986	0.962	0.968	0.954	0.987
	X^2	0.893	1	0.826	1	0.986	1
	SSE	6.311	15.183	5.223	13.59	0.177	0.640
	ABS	3.312	0.502	3.756	0.577	1.042	0.158
	ARE	65.454	24.455	75.963	20.839	95.393	56.663
Temkin	R^2	0.783	0.783	0.912	0.912	0.972	0.972
	X^2	0.783	0.701	0.293	0.958	0.897	0.999
	SSE	0.025	18.922	27.379	15.843	1.33	0.693
	ABS	32.24	2.036	4.432	1.2	1.174	0.231
	ARE	239.701	24.455	166.445	70.823	193.188	67.984
D-R	R^2	0.553	0.925	0.609	0.974	0.8	0.973
	X^2	0.553	0.998	0.988	0.998	0.99	1
	SSE	0.963	17.147	8.695	14.791	0.192	0.640
	ABS	8.226	0.883	2.105	0.703	0.981	0.108
	ARE	53.653	49.691	39.471	35.56	88.828	25.697

Table 6. *Lead, copper and cadmium isotherm models linear and nonlinear parameters*

Model	Parameters	Pb		Cu		Cd	
		Linear	**Nonlinear**	**Linear**	**Nonlinear**	**Linear**	**Nonlinear**
Langmuir Type I	Q_{max} (mg/g)	1.59	7.27	1.18	1.45	0.24	0.26
	K_L (L/mg)	0.38	0.03	0.43	0.15	1.07	0.68
	R_L	0.55-0.94	0.10-0.58	0.14-0.81	0.05-0.59	0.10-0.79	0.07-0.70
	R^2	0.923	0.987	0.943	0.981	0.991	0.999
Freundlich	K_F(mg/g).(L/mg)$^{(1/n)}$	0.14	0.24	2.47	0.41	0.004	0.15
	N	2.04	1.09	0.08	3.30	2.31	6.09
	R^2	0.953	0.986	0.962	0.968	0.954	0.987
Temkin	B_T (J/mol)	0.22	0.16	0.18	0.12	0.04	0.03
	A_T (L/g)	704.12	354.66	525.05	398.13	1561.52	974.9
	R^2	0.783	0.783	0.912	0.912	0.972	0.972
D-R	β(mol^2/kJ^2)	0.03	0.67	0.04	2.67	0.04	0.23
	Q_{max}(mol/g)	0.48	1.35	0.55	1.15	0.02	0.22
	E(kJ/mol)	4.07	0.86	3.48	0.43	3.68	1.47
	R^2	0.553	0.925	0.609	0.974	0.800	0.973

Table 7. *Kinetic model error functions of with linear and nonlinear regression*

Model		Pb		Cu		Cd	
		Linear	**Nonlinear**	**Linear**	**Nonlinear**	**Linear**	**Nonlinear**
PFO	R^2	0.942	0.950	0.899	0.942	0.843	0.892
	X^2	1.000	1.000	1.000	0.984	0.240	0.000
	SSE	34.156	30.888	21.290	14.093	0.974	0.613
	ABS	0.645	1.015	0.986	2.375	1.890	2.492
	ARE	17.444	17.174	27.637	45.993	85.162	102.999
PSO	R^2	0.950	0.950	0.918	0.940	0.625	0.680
	X^2	1.000	1.000	1.000	0.933	1.000	0.999
	SSE	32.915	32.522	19.736	12.459	2.192	1.539
	ABS	0.605	0.662	0.778	2.977	0.461	0.965
	ARE	14.923	15.298	20.320	53.996	23.784	46.472
Elovich	R^2	0.950	0.952	0.862	0.939	0.702	0.892
	X^2	0.989	1.000	0.972	0.045	1.000	0.000
	SSE	50.355	32.278	33.483	8.032	1.903	0.613
	ABS	5.066	0.965	5.410	4.883	0.333	2.491
	ARE	127.619	31.310	165.581	80.483	13.577	102.983

Table 8. *Kinetic models parameters and coefficients of determination*

Model	Parameters	Pb		Cu		Cd	
		Linear	**Nonlinear**	**Linear**	**Nonlinear**	**Linear**	**Nonlinear**
PFP	Q_e (mg/g)	1.46	1.46	1.32	1.32	0.22	0.67
	k_1 (1/min)	0.01	1.00E-02	0.01	4.14E-03	3.45E-03	7.61E-08
	R^2	0.942	0.950	0.899	0.942	0.843	0.889
PSO	Q_e (mg/g)	1.93	1.93	1.80	1.80	0.39	0.30
	k_2 (g.mg^{-1}*min^{-1})	5.60E-03	5.43E-03	3.90E-03	1.48E-03	0.06	0.05
	R^2	0.950	0.950	0.918	0.940	0.625	0.680
Elovich	Q_e (mg/g)	0.20	0.05	0.19	2.29E-03	0.05	6.10E-07
	k_e (1/min)	2.62	2.61	3.16	3.15	19.31	0.03
	R^2	0.950	0.952	0.862	0.939	0.702	0.892